Prescribed Performance Control for Signal Temporal Logic Specifications

Lars Lindemann, Christos K. Verginis, and Dimos V. Dimarogonas

***Abstract*— Motivated by the recent interest in formal methods-based control for dynamic robots, we discuss the applicability of prescribed performance control to nonlinear systems subject to signal temporal logic specifications. Prescribed performance control imposes a desired transient behavior on the system trajectories that is leveraged to satisfy atomic signal temporal logic specifications. A hybrid control strategy is then used to satisfy a finite set of these atomic specifications. Simulations of a multi-agent system, using consensus dynamics, show that a wide range of specifications, i.e., formation, sequencing, and dispersion, can be robustly satisfied.**

I. INTRODUCTION

Temporal logics have lately gained much attention in robotic applications due to the possibility of formulating complex temporal specifications leading to formal methods-based control strategies [1]. These logics have for instance been used in multi-agent systems to perform realistic real-world tasks such as sequencing, coverage, surveillance, and formation control. In this multi-agent setup, linear temporal logic (LTL) [2] and metric interval temporal logic (MITL) [3] have been used. These approaches abstract the physical environment, including robot dynamics, and the temporal logic formula into a finite-state automaton representing all possible robot motions. Search algorithms are then used to find a formula-satisfying discrete path that is subsequently accomplished by continuous control laws. However, these approaches may be subject to the state-space explosion problem [4, Section 2.3].

Prescribed performance control (PPC) [5] explicitly takes the transient and steady-state behavior of a tracking error into account. A user-defined performance function prescribes a desired temporal behavior that is then achieved by a continuous state feedback control law.

Signal temporal logic (STL) [6] is a predicate logic, which uses quantitative time properties and entails the definition of a robustness measure, called space robustness [7]. This measure indicates if a formula is marginally or greatly satisfied by a signal. STL was introduced in the context of monitoring, but not control. Control of systems subject to STL is a difficult task due to the nonlinear, nonconvex, noncausal, and nonsmooth semantics. Previous work on STL control synthesis has been considered [8], [9], [10] by using model predictive control (MPC), while [11] explicitly considers multi-agent systems. In this paper, we consider a nonlinear system subject to a subset of STL. We recast this constrained control problem into a PPC framework to satisfy atomic temporal formulas. Subsequently, the hybrid system framework in [12] is used to satisfy a finite set of these atomic temporal formulas. To the best of the authors' knowledge, the approach presented in this paper is the first approach using a continuous state feedback control law.

The remainder of this paper is organized as follows: Section II introduces notation and preliminaries. Section III illustrates the underlying main idea and the problem definition. Section IV presents a control law satisfying atomic temporal formulas, while Section V considers a finite set of these atomic temporal formulas. Section VI presents simulations of a centralized multi-agent system subject to STL formulas, followed by a conclusion in Section VII.

II. NOTATION AND PRELIMINARIES

Scalars are denoted by lowercase, non-bold letters x and column vectors are lowercase, bold letters $\boldsymbol{x}$. The vector $\boldsymbol{0}_n$ consists of n zeros. True and false are denoted by $\top$ and $\bot$ with $\mathbb{B} := \{\top, \bot\}$; $\mathbb{R}^n$ is the n-dimensional vector space over the real numbers $\mathbb{R}$. The natural, non-negative, and positive real numbers are $\mathbb{N}$, $\mathbb{R}_{\geq 0}$, and $\mathbb{R}_{>0}$, respectively.

Let $\boldsymbol{x} \in \mathbb{R}^n$, $\boldsymbol{u} \in \mathbb{R}^m$, and $\boldsymbol{w} \in \mathcal{W}$ be the state, input, and additive noise of a nonlinear system

$$\dot{\boldsymbol{x}} = f(\boldsymbol{x}) + g(\boldsymbol{x})\boldsymbol{u} + \boldsymbol{w}, \tag{1}$$

where $\mathcal{W} \subset \mathbb{R}^n$ is a bounded set.

Assumption 1: The functions $f : \mathbb{R}^n \to \mathbb{R}^n$ and $g : \mathbb{R}^n \to \mathbb{R}^{n\times m}$ are locally Lipschitz continuous, and $g(\boldsymbol{x})g^T(\boldsymbol{x})$ is positive definite for all $\boldsymbol{x} \in \mathbb{R}^n$.

A. Signal Temporal Logic (STL)

Signal temporal logic [6] is a predicate logic based on continuous-time signals. STL consists of predicates μ that are obtained after evaluation of a function $h : \mathbb{R}^n \to \mathbb{R}$ as $\mu := \begin{cases} \top \text{ if } h(\boldsymbol{x}) \geq 0 \\ \bot \text{ if } h(\boldsymbol{x}) < 0. \end{cases}$ For instance, consider the predicate $\mu := (x \geq 1)$, which can be expressed by $h(x) := x - 1$. The STL syntax is given by

$$\phi \ ::= \ \top \mid \mu \mid \neg\phi \mid \phi_1 \wedge \phi_2 \mid \phi_1 \, \mathcal{U}_{[a,b]} \, \phi_2 \ ,$$

where μ is a predicate and ϕ_1, ϕ_2 are STL formulas. The temporal until-operator $\mathcal{U}_{[a,b]}$ is time bounded with time interval $[a, b]$ where $a, b \in \mathbb{R}_{\geq 0} \cup \infty$ such that $a \leq b$. Let

This work was supported in part by the Swedish Research Council (VR), the European Research Council (ERC), the Swedish Foundation for Strategic Research (SSF), the EU H2020 Co4Robots project, and the Knut and Alice Wallenberg Foundation (KAW).

The authors are with the Department of Automatic Control, School of Electrical Engineering, Royal Institute of Technology (KTH), 100 44 Stockholm, Sweden. llindem@kth.se (L. Lindemann), cverginis@kth.se (C.K. Verginis), dimos@kth.se (D.V. Dimarogonas)

$(\boldsymbol{x}, t) \models \phi$ denote the satisfaction relation, i.e., if a signal $\boldsymbol{x}: \mathbb{R}_{\geq 0} \to \mathbb{R}^n$, possibly a solution of (1) with $\boldsymbol{x}_0 := \boldsymbol{x}(0)$, satisfies ϕ at time t. The semantics of STL are $(\boldsymbol{x}, t) \models \mu$ if and only if $h(\boldsymbol{x}(t)) \geq 0$, $(\boldsymbol{x}, t) \models \neg\mu$ if and only if $\neg((\boldsymbol{x}, t) \models \mu)$, $(\boldsymbol{x}, t) \models \phi_1 \wedge \phi_2$ if and only if $(\boldsymbol{x}, t) \models \phi_1 \wedge (\boldsymbol{x}, t) \models \phi_2$, and $(\boldsymbol{x}, t) \models \phi_1 \mathcal{U}_{[a,b]}\, \phi_2$ if and only if $\exists t_1 \in [t+a, t+b]$ s.t. $(\boldsymbol{x}, t_1) \models \phi_2 \wedge \forall t_2 \in [t, t_1], (\boldsymbol{x}, t_2) \models \phi_1$. The disjunction-, eventually-, and always-operator can be derived as $\phi_1 \vee \phi_2 = \neg(\neg\phi_1 \wedge \neg\phi_2)$, $F_{[a,b]}\phi = \top \mathcal{U}_{[a,b]}\, \phi$, and $G_{[a,b]}\phi = \neg F_{[a,b]}\neg\phi$. Space robustness $\rho^\phi(\boldsymbol{x}, t)$ [7] are robust semantics for STL, given in Definition 1, for which it holds that $(\boldsymbol{x}, t) \models \phi$ if $\rho^\phi(\boldsymbol{x}, t) > 0$.

Definition 1: [7, Definition 3] The semantics of space robustness are recursively given by:

$$\begin{aligned}
\rho^{\mu}(\boldsymbol{x}, t) &:= h(\boldsymbol{x}(t)) \\
\rho^{\neg\phi}(\boldsymbol{x}, t) &:= -\rho^{\phi}(\boldsymbol{x}, t) \\
\rho^{\phi_1 \wedge \phi_2}(\boldsymbol{x}, t) &:= \min\big(\rho^{\phi_1}(\boldsymbol{x}, t), \rho^{\phi_2}(\boldsymbol{x}, t)\big) \\
\rho^{F_{[a,b]}\phi}(\boldsymbol{x}, t) &:= \max_{t_1 \in [t+a, t+b]} \rho^{\phi}(\boldsymbol{x}, t_1) \\
\rho^{G_{[a,b]}\phi}(\boldsymbol{x}, t) &:= \min_{t_1 \in [t+a, t+b]} \rho^{\phi}(\boldsymbol{x}, t_1).
\end{aligned}$$

The definitions of $\rho^{\phi_1 \vee \phi_2}(\boldsymbol{x}, t)$ and $\rho^{\phi_1 \mathcal{U}_{[a,b]}\, \phi_2}(\boldsymbol{x}, t)$ are omitted due to space limitations. We abuse the notation as $\rho^\phi\big(\boldsymbol{x}(t)\big) := \rho^\phi(\boldsymbol{x}, t)$ if t is not explicitly contained in $\rho^\phi(\boldsymbol{x}, t)$. For instance, $\rho^\mu\big(\boldsymbol{x}(t)\big) := \rho^\mu(\boldsymbol{x}, t) := h(\boldsymbol{x}(t))$ since $h(\boldsymbol{x}(t))$ does not contain t as an explicit parameter. However, t is explicitly contained in $\rho^\phi(\boldsymbol{x}, t)$ if temporal operators (eventually, always, or until) are used. In this paper, conjunctions are approximated by smooth functions.

Assumption 2: The non-smooth conjunction $\rho^{\phi_1 \wedge \phi_2}(\boldsymbol{x}, t)$ in Definition 1 is approximated by a smooth function as $\rho^{\phi_1 \wedge \phi_2}(\boldsymbol{x}, t) \approx -\ln\big(\exp(-\rho^{\phi_1}(\boldsymbol{x}, t)) + \exp(-\rho^{\phi_2}(\boldsymbol{x}, t))\big)$.

Remark 1: The aforementioned approximation is an under-approximation of the robust semantics in Definition 1, i.e., $-\ln\big(\exp(-\rho^{\phi_1}(\boldsymbol{x}, t)) + \exp(-\rho^{\phi_2}(\boldsymbol{x}, t))\big) \leq \min\big(\rho^{\phi_1}(\boldsymbol{x}, t), \rho^{\phi_2}(\boldsymbol{x}, t)\big)$. This means that $(\boldsymbol{x}, t) \models \phi_1 \wedge \phi_2$ if $-\ln\big(\exp(-\rho^{\phi_1}(\boldsymbol{x}, t)) + \exp(-\rho^{\phi_2}(\boldsymbol{x}, t))\big) > 0$.

B. Prescribed Performance Control (PPC)

Prescribed performance control (PPC) [5] constrains a tracking error $\boldsymbol{e}: \mathbb{R}_{\geq 0} \to \mathbb{R}^n$ to a funnel. For instance, consider $\boldsymbol{e}(t) := \boldsymbol{x}(t) - \boldsymbol{x}_d(t)$ where $\boldsymbol{x}_d: \mathbb{R}_{\geq 0} \to \mathbb{R}^n$ is a desired trajectory. To prescribe transient and steady-state behavior to this error, we define the performance function γ.

Definition 2: [5] A performance function $\gamma: \mathbb{R}_{\geq 0} \to \mathbb{R}_{>0}$ is a continuously differentiable, bounded, positive, and non-increasing function. We define $\gamma(t) := (\gamma_0 - \gamma_\infty)\exp(-lt) + \gamma_\infty$ where $\gamma_0, \gamma_\infty \in \mathbb{R}_{>0}$ with $\gamma_0 \geq \gamma_\infty$ and $l \in \mathbb{R}_{\geq 0}$.

The task is to synthesize a feedback control law such that, given $-\gamma_i(0) < e_i(0) < M\gamma_i(0)$, the errors e_i satisfy

$$-\gamma_i(t) < e_i(t) < M\gamma_i(t) \quad \forall t \in \mathbb{R}_{\geq 0}, \forall i \in \{1, \ldots, n\} \quad (2)$$

with $0 \leq M \leq 1$ and γ_i being a performance function as in Definition 2; γ_i is a design parameter by which transient and steady-state behavior of e_i can be prescribed. Similar to M in the right inequality of (2), another constant could be added to the left inequality, which however will not be considered here. Next, define the normalized error $\xi_i := \frac{e_i}{\gamma_i}$ and the transformation function S in Definition 3.

Definition 3: [5] Let $S: (-1, M) \to \mathbb{R}$ be a strictly increasing function, hence injective and admitting an inverse. In particular, we define $S(\xi) := \ln\Big(-\frac{\xi+1}{\xi-M}\Big)$.

Dividing (2) by γ_i and applying the transformation function S results in an unconstrained control problem $-\infty < S\big(\xi_i(t)\big) < \infty$ with the transformed error $\epsilon_i := S\big(\xi_i\big)$. If $\epsilon_i(t)$ is bounded for all $t \in \mathbb{R}_{\geq 0}$, then e_i satisfies (2). This is a consequence of the fact that S admits an inverse.

III. Casting STL Control into a PPC Framework

In this paper, the following STL subset is considered

$$\psi \;::=\; \top \mid \mu \mid \neg\mu \mid \psi_1 \wedge \psi_2 \quad (3a)$$

$$\phi \;::=\; G_{[a,b]}\psi \mid F_{[a,b]}\psi \quad (3b)$$

$$\theta^{s_1} ::= \bigwedge_{i=1}^{N} \phi_i \text{ with } b_n \leq a_{n+1},\ \forall n \in \{1, \ldots, N-1\} \quad (3c)$$

$$\theta^{s_2} ::= F_{[c_1,d_1]}\Big(\psi_1 \wedge F_{[c_2,d_2]}\big(\psi_2 \wedge F_{[c_3,d_3]}(\ldots \wedge \phi_N)\big)\Big) \quad (3d)$$

$$\theta ::= \theta^{s_1} \mid \theta^{s_2}, \quad (3e)$$

where μ is a predicate and ψ_1, ψ_2 are formulas of class ψ, whereas ϕ_i with $i \in \{1, \ldots, N\}$ are formulas of class ϕ with time intervals $[a_i, b_i]$. We refer to ψ as non-temporal formulas. Due to the previous discussion, we write $\rho^\psi\big(\boldsymbol{x}(t)\big) := \rho^\psi(\boldsymbol{x}, t)$ and sometimes even omit t resulting in $\rho^\psi(\boldsymbol{x})$. In contrast, ϕ and θ are referred to as temporal formulas due to the use of always- and eventually-operators. We further refer to formulas (3b) by the term atomic temporal formulas, while formulas in (3e) are denoted as sequential formulas. Note that (3e) either consists of (3c) or (3d).

Assumption 3: Each formula of class ψ that is contained in (3b), (3c), and (3d) is: 1) s.t. $\rho^\psi(\boldsymbol{x})$ is concave and 2) well-posed in the sense that $(\boldsymbol{x}, 0) \models \psi$ implies $\|\boldsymbol{x}(0)\| < \infty$.

Remark 2: Part 2) of Assumption 3 is not restrictive since $\psi_{Ass.3} := (\|\boldsymbol{x}\| < c)$, where c is a sufficiently large positive constant, can be combined with the desired ψ so that $\psi \wedge \psi_{Ass.3}$ is well-posed.

The first objective in this paper is to synthesize a continuous feedback control law $\boldsymbol{u}(\boldsymbol{x}, t)$ for atomic temporal formulas ϕ in (3b) such that $\rho^\phi(\boldsymbol{x}, 0) > r$ where $r \in \mathbb{R}_{\geq 0}$ is a robustness measure and $\boldsymbol{x}: \mathbb{R}_{\geq 0} \to \mathbb{R}^n$ is the closed-loop solution of (1) with initial condition $\boldsymbol{x}_0$. Additionally, we will upper bound $\rho^\phi(\boldsymbol{x}, 0) < \rho_{max}$ with $\rho_{max} \in \mathbb{R}_{>0}$. For ϕ in (3b) with the corresponding ψ, we achieve $r < \rho^\phi(\boldsymbol{x}, 0) < \rho_{max}$ by prescribing a temporal behavior to $\rho^\psi\big(\boldsymbol{x}(t)\big)$ through the design parameters γ and ρ_{max} as

$$-\gamma(t) + \rho_{max} < \rho^\psi\big(\boldsymbol{x}(t)\big) < \rho_{max}. \quad (4)$$

The connection between the non-temporal $\rho^\psi\big(\boldsymbol{x}(t)\big)$ and the temporal $\rho^\phi(\boldsymbol{x}, 0)$ is made by the performance function γ. In fact, γ prescribes temporal behavior that, in combination with $\rho^\psi\big(\boldsymbol{x}(t)\big)$, mimics $\rho^\phi(\boldsymbol{x}, 0)$ as illustrated next.

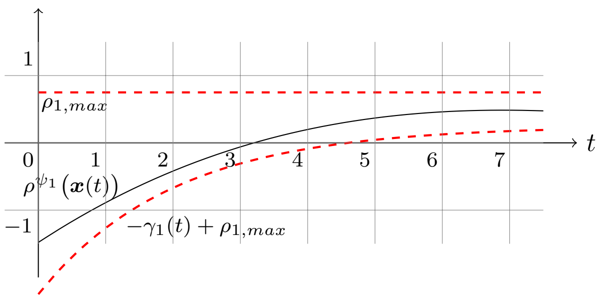

(a) Funnel for $\phi_1 = F_{[0,\infty)}\psi_1$ s.t. $\rho^{\phi_1}(\boldsymbol{x},0) > r$ with $r := 0$

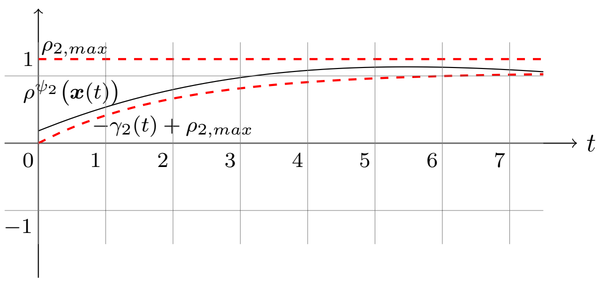

(b) Funnel for $\phi_2 = G_{[0,\infty)}\psi_2$ s.t. $\rho^{\phi_2}(\boldsymbol{x},0) > r$ with $r := 0$

Fig. 1: Connection between $\rho^{\psi}\big(\boldsymbol{x}(t)\big)$ and $\rho^{\phi}(\boldsymbol{x},0)$

Example 1: Fig. 1a visualizes the idea for the eventually-operator $\phi_1 := F_{[0,\infty)}\psi_1$, while Fig. 1b expresses the always-operator $\phi_2 := G_{[0,\infty)}\psi_2$. Note that these figures show the funnel in (4), hence imposing prescribed temporal behavior on $\rho^{\psi}\big(\boldsymbol{x}(t)\big)$. It is easy to verify that if $\rho^{\psi_1}\big(\boldsymbol{x}(t)\big) \in (-\gamma_1(t)+\rho_{1,max}, \rho_{1,max})$ and $\rho^{\psi_2}\big(\boldsymbol{x}(t)\big) \in (-\gamma_2(t)+\rho_{2,max}, \rho_{2,max})$ for all $t \in \mathbb{R}_{\geq 0}$ as in Fig. 1, i.e. (4) is satisfied, then ϕ_1 and ϕ_2 are satisfied. For instance, in Fig. 1a the lower funnel $-\gamma_1(t)+\rho_{1,max}$ forces $\rho^{\psi_1}\big(\boldsymbol{x}(t)\big) > r := 0$ by no later than approximately 4.5 time units. Thus, the formulas $\phi_1 := F_{[0,\infty)}\psi_1$ or also $\phi_3 := F_{[2,5]}\psi_1$ are satisfied, which means that $\rho^{\phi_1}(\boldsymbol{x},0) > 0$ and $\rho^{\phi_3}(\boldsymbol{x},0) > 0$.

The choice of the design parameters γ, ρ_{max}, and r will be discussed in Section IV. Therefore, define the global optimum of $\rho^{\psi}(\boldsymbol{x})$ as $\rho^{\psi}_{opt} := \sup_{\boldsymbol{x}\in\mathbb{R}^n} \rho^{\psi}(\boldsymbol{x})$; $\rho^{\psi}(\boldsymbol{x})$ is continuous and concave due to Assumption 2 and 3, which makes the calculation of ρ^{ψ}_{opt} straightforward. If $\rho^{\psi}_{opt} > 0$, it holds that ϕ is feasible, i.e., $\exists \boldsymbol{x} : \mathbb{R}_{\geq 0} \to \mathbb{R}^n$ s.t. $(\boldsymbol{x},0) \models \phi$.

Assumption 4: The optimum of $\rho^{\psi}(\boldsymbol{x})$ is s.t. $\rho^{\psi}_{opt} > 0$.

Equation (4) can now be written as

$$-\gamma(t) < \rho^{\psi}\big(\boldsymbol{x}(t)\big) - \rho_{max} < 0, \tag{5}$$

which resembles (2) by defining the one-dimensional error $e(\boldsymbol{x}) := \rho^{\psi}(\boldsymbol{x}) - \rho_{max}$ and $M := 0$. The normalized error is defined as $\xi(\boldsymbol{x},t) := \frac{e(\boldsymbol{x})}{\gamma(t)}$, while the transformed error is

$$\epsilon(\boldsymbol{x},t) := S\big(\xi(\boldsymbol{x},t)\big) = \ln\Big(-\frac{\xi(\boldsymbol{x},t)+1}{\xi(\boldsymbol{x},t)}\Big). \tag{6}$$

As a notational rule, when talking about the solution $\boldsymbol{x}(t)$ of (1) at time t, we use $e(t)$, $\xi(t)$, and $\epsilon(t)$, while we use $e(\boldsymbol{x})$, $\xi(\boldsymbol{x},t)$, and $\epsilon(\boldsymbol{x},t)$ when we talk about $\boldsymbol{x}$ as a state. Hence, (5) can be written as $-\gamma(t) < e(t) < 0$, which in turn leads to $-1 < \xi(t) < 0$. Applying the transformation function S to this inequality finally results in $-\infty < \epsilon(t) < \infty$. In order to have a feasible problem, the condition $\xi\big(\boldsymbol{x}(0),0\big) \in \Omega_\xi := (-1,0)$ needs to hold.

The second objective in this paper is to consider sequential formulas θ as in (3e). Therefore, the hybrid system framework of [12] will be used. The problem definition is now:

Problem 1: Consider the system given in (1) subject to a STL formula θ as in (3e). Design a piecewise-continuous feedback control law $\boldsymbol{u}(\boldsymbol{x},t)$ such that $0 \leq r < \rho^{\theta}(\boldsymbol{x},0) < \rho_{max}$, i.e., $(\boldsymbol{x},0) \models \theta$.

Our problem solution consists of a three-step procedure: First, a continuous feedback control law $\boldsymbol{u}(\boldsymbol{x},t)$ is designed in Theorem 1 such that (4) is satisfied. Second, γ is designed in Theorem 2 such that $r < \rho^{\phi}(\boldsymbol{x},0) < \rho_{max}$ if $\boldsymbol{u}(\boldsymbol{x},t)$ from Theorem 1 is used. Third, Theorem 3 states a hybrid control strategy such that $r < \rho^{\theta}(\boldsymbol{x},0) < \rho_{max}$.

IV. Control Law for Atomic Temporal Formulas

We first derive a control law $\boldsymbol{u}(\boldsymbol{x},t)$ in the next theorem such that $\rho^{\psi}\big(\boldsymbol{x}(t)\big)$ satisfies (4) with $\epsilon(\boldsymbol{x},t)$ as in (6).

Theorem 1: Consider the system (1) and a formula ϕ as in (3b) with the corresponding ψ. If $\xi\big(\boldsymbol{x}_0,0\big) \in \Omega_\xi := (-1,0)$, $\rho_{max} \in \big(\max\big(0,\rho^{\psi}(\boldsymbol{x}_0)\big),\rho^{\psi}_{opt}\big)$, and Assumptions 1-4 are satisfied, then the control law

$$\boldsymbol{u}(\boldsymbol{x},t) := -\epsilon(\boldsymbol{x},t)g^T(\boldsymbol{x})\frac{\partial\rho^{\psi}(\boldsymbol{x})}{\partial\boldsymbol{x}} \tag{7}$$

guarantees that (4) is satisfied for all $t \in \mathbb{R}_{\geq 0}$ with all closed-loop signals being well-posed, i.e., continuous and bounded.

Proof: The proof can be found in [13]. ■

Next, γ is designed such that the control law (7) results in $0 \leq r < \rho^{\phi}(\boldsymbol{x},0) < \rho_{max}$. Define the variable

$$t_* \in \begin{cases} a & \text{if } \phi = G_{[a,b]}\psi \\ [a,b] & \text{if } \phi = F_{[a,b]}\psi. \end{cases} \tag{8}$$

Our goal is to enforce $r < \rho^{\psi}\big(\boldsymbol{x}(t)\big) < \rho_{max}$ for all $t \geq t_*$ by the choice of γ. This will lead to $r < \rho^{\phi}(\boldsymbol{x},0) < \rho_{max}$ by the choice of t_*. We select $r \in [0,\rho_{max})$ and define feasibility of a formula ϕ with respect to r, $\boldsymbol{x}_0$, and t_*.

Definition 4: A formula ϕ as in (3b) is feasible with respect to r, $\boldsymbol{x}_0$, and t_* if and only if: 1) $t_* > 0$ or 2) $t_* = 0$ and $\rho^{\psi}(\boldsymbol{x}_0) > r$.

For the design of γ assume that ϕ is feasible w.r.t. r, $\boldsymbol{x}_0$, and t_* and recall that $\gamma(t) := (\gamma_0 - \gamma_\infty)\exp(-lt) + \gamma_\infty$. The crucial part of Theorem 1 is the assumption that $\xi(\boldsymbol{x}_0,0) \in \Omega_\xi$. It is possible to choose γ_0 such that $\xi(\boldsymbol{x}_0,0) \in \Omega_\xi$, which is equivalent to $-1 < \frac{\rho^{\psi}(\boldsymbol{x}_0)-\rho_{max}}{\gamma(0)} < 0$. It should also hold that $-\gamma_0 + \rho_{max} \geq r$ if $t_* = 0$ due to (4) and since we want $r < \rho^{\psi}\big(\boldsymbol{x}(t)\big)$ for all $t \geq t_*$. This is illustrated in Fig. 1b with $t_* = 0$ (since $\phi_2 = G_{[0,\infty)}\psi_2$) and $r := 0$ and where it should hence hold that $-\gamma_0 + \rho_{max} \geq 0$ is satisfied as indicated by the dashed line. To conclude, γ_0 is

$$\gamma_0 \in \begin{cases} \big(\rho_{max} - \rho^{\psi}(\boldsymbol{x}_0),\infty\big) & \text{if } t_* > 0 \\ \big(\rho_{max} - \rho^{\psi}(\boldsymbol{x}_0),\rho_{max} - r\big] & \text{if } t_* = 0. \end{cases} \tag{9}$$

At $t = \infty$, it is required that $\max(-\gamma_0 + \rho_{max}, r) \leq -\gamma_\infty + \rho_{max} < \rho_{max}$, where the left inequality enforces that $-\gamma + \rho_{max}$ is a non-decreasing function, which in turn leads to γ being non-increasing. The right inequality stems from (4). Therefore, we set

$$\gamma_\infty \in \Big(0, \min\big(\gamma_0, \rho_{max} - r\big)\Big]. \tag{10}$$

For the calculation of l, three cases need to be distinguished: 1) $\rho^\psi(\boldsymbol{x}_0) > r$, 2) $\rho^\psi(\boldsymbol{x}_0) \leq r$ and $t_* > 0$, and 3) $\rho^\psi(\boldsymbol{x}_0) \leq r$ and $t_* = 0$. Case 3) can be excluded since ϕ is assumed to be feasible w.r.t. r, $\boldsymbol{x}_0$, and t_*. Next, select l as

$$l \in \begin{cases} \mathbb{R}_{\geq 0} & \text{if } -\gamma_0 + \rho_{max} \geq r \\ -\frac{\ln\left(\frac{r+\gamma_\infty - \rho_{max}}{-(\gamma_0 - \gamma_\infty)}\right)}{t_*} & \text{if } -\gamma_0 + \rho_{max} < r, t_* > 0, \end{cases} \tag{11}$$

which ensures that $-\gamma(t_*) + \rho_{max} \geq r$. Under (7), this consequently leads to $\rho^\psi\big(\boldsymbol{x}(t)\big) > r$ for all $t \geq t_*$ since γ is non-increasing.

Theorem 2: Consider the system (1) and a formula ϕ as in (3b). If Assumptions 1-4 hold, $r \in [0, \rho_{max})$, the control law in (7) is used, and ϕ is feasible w.r.t. r, $\boldsymbol{x}_0$, and t_*, then choosing γ_0, γ_∞, and l as in (9), (10), and (11), respectively, ensures that $0 \leq r < \rho^\phi(\boldsymbol{x}, 0) < \rho_{max}$, i.e., $(\boldsymbol{x}, 0) \models \phi$.

Proof: The proof can be found in [13]. ■

V. CONTROL STRATEGY FOR SEQUENTIAL FORMULAS

In this section, we develop a hybrid control strategy for sequential formulas θ as in (3e), which either correspond to θ^{s_1} or θ^{s_2} as in (3c) or (3d), respectively. Note that both of these consist of N atomic temporal formulas: θ^{s_1} entails N atomic temporal formulas ϕ_i with $[a_i, b_i]$ for all $i \in \{1, \ldots, N\}$. Similarly, θ^{s_2} boils down to $N-1$ atomic temporal formulas $\phi_i = F_{[a_i,b_i]}\psi_i$ with $i \in \{1, \ldots, N-1\}$, $a_i := \sum_{k=1}^{i} c_k$, $b_i := \sum_{k=1}^{i} d_k$, and ϕ_N. For instance, $F_{[c_1,d_1]}\big(\psi_1 \wedge F_{[c_2,d_2]}(\psi_2 \wedge F_{[c_3,d_3]}\psi_3)\big)$ is satisfied if and only if $F_{[c_1,d_1]}\psi_1 \wedge F_{[c_1+c_2,d_1+d_2]}\psi_2 \wedge F_{[c_1+c_2+c_3,d_1+d_2+d_3]}\psi_3 := F_{[a_1,b_1]}\psi_1 \wedge F_{[a_2,b_2]}\psi_2 \wedge F_{[a_3,b_3]}\psi_3$ is satisfied. To conclude, θ consists of N atomic temporal formulas ϕ_i with $i \in \{1, \ldots, N\}$. Each ϕ_i entails a robustness function denoted by $\rho^{\psi_i}(\boldsymbol{x})$ and corresponding design parameters $t_{i,*}$, r_i, $\rho_{i,max}$, and $\gamma_i(t) = (\gamma_{i,0} - \gamma_{i,\infty})\exp(-l_i t) + \gamma_{i,\infty}$ in accordance with t_*, r, ρ_{max}, and γ in Section IV. Each ϕ_i will be processed one at a time. If ϕ_i has been satisfied, the next atomic temporal formula ϕ_{i+1} becomes active and a switch takes place. Denote the time sequence of these switching times by $\{\Delta_1 := 0, \Delta_2, \ldots, \Delta_N\}$ where $\Delta_i \leq \Delta_{i+1}$. Note that $t_{i,*}$, r_i, $\rho_{i,max}$, $\gamma_{i,0}$, $\gamma_{i,\infty}$, and l_i need to be calculated during runtime at each switching time Δ_i. Furthermore, set

$$p := \begin{cases} 1 \text{ if } \theta = \theta^{s_1} \\ 0 \text{ if } \theta = \theta^{s_2} \end{cases} \text{ and } m_i := \begin{cases} 1 \text{ if } \phi_i = G_{[a_i,b_i]}\psi_i \\ 0 \text{ if } \phi_i = F_{[a_i,b_i]}\psi_i. \end{cases}$$

A hybrid control strategy in the framework introduced in Definition 5 will be used to process each ϕ_i sequentially.

Definition 5: [12] A hybrid system is a tuple $\mathcal{H} := (C, F, D, G)$, where C, D, F, and G are the flow and jump set and the possibly set-valued flow and jump map, respectively. The discrete and continuous dynamics are

$$\begin{cases} \dot{\boldsymbol{z}} \in F(\boldsymbol{z}) & \text{if } \boldsymbol{z} \in C \\ \boldsymbol{z}^+ \in G(\boldsymbol{z}) & \text{if } \boldsymbol{z} \in D. \end{cases}$$

Define $\boldsymbol{p}_f := \begin{bmatrix} t_* & r & \rho_{max} & \gamma_0 & \gamma_\infty & l \end{bmatrix}^T$, gathering all parameters defining the funnel in (4), and the hybrid state $\boldsymbol{z} := \begin{bmatrix} q & \boldsymbol{x}^T & t & \Delta & \boldsymbol{p}_f^T \end{bmatrix}^T \in \{1, \ldots, N+1\} \times \mathbb{R}^n \times \mathbb{R}^8_{\geq 0} =: \mathcal{Z}$. Note that Δ is the value of the latest switching time. In adherence to the terminology in [12], we interchangeably call switches jumps. The discrete state q indicates which formula ϕ_q is currently active, while $q = N+1$ indicates the final discrete state when θ has already been satisfied. In the proof of Theorem 1, it was shown that $\boldsymbol{x}(t) \in \Omega'_{\boldsymbol{x}}$ for all $t \in \mathbb{R}_{\geq 0}$, where $\Omega'_{\boldsymbol{x}}$ is a compact set. Let $\Omega'_{q,\boldsymbol{x}}$ denote $\Omega'_{\boldsymbol{x}}$ corresponding to the formula ϕ_q. Next, define the sets $\mathcal{X}_q := \{\boldsymbol{x} \in \mathbb{R}^n | r_q < \rho^{\psi_q}(\boldsymbol{x}) < \rho_{q,max}\}$ and $\mathcal{Y}_q := [0, {b_q}^p + \big(\sum_{i=1}^{q} d_i\big)^{1-p} - 1] \times t_{q,*} \times r_q \times \rho_{q,max} \times \gamma_{q,0} \times \gamma_{q,\infty} \times l_q$. Note that p determines if $[a_q, b_q]$ or $[c_q, d_q]$ is used. For all $q \in \{1, \ldots, N\}$ and similarly to (8), set

$$t_{q,*} \in \begin{cases} a_q & \text{if } p = 1, m_q = 1 \\ [a_q, b_q] & \text{if } p = 1, m_q = 0 \\ c_q & \text{if } p = 0, m_q = 1 \\ [c_q, d_q] & \text{if } p = 0, m_q = 0. \end{cases} \tag{12}$$

Define the set $\mathcal{D}_q$ that indicates satisfaction of ϕ_q and leads to a jump to process ϕ_{q+1}. For $q \in \{1, \ldots, N\}$, we have

$$\mathcal{D}_q := \begin{cases} q \times \mathcal{X}_q \times ({b_q}^p + {d_q}^{1-p} - 1 - p\Delta) \times \mathcal{Y}_q & \text{if } m_q = 1 \\ q \times \mathcal{X}_q \times ([{a_q}^p + {c_q}^{1-p} - 1, t_{q,*}] - p\Delta) \times \mathcal{Y}_q & \text{else,} \end{cases}$$

which indicates that $\rho^{\phi_q}(\boldsymbol{x}, \Delta_q) > r_q$ if $\boldsymbol{z} \in \mathcal{D}_q$. This follows since $\boldsymbol{x} \in \mathcal{X}_q$ at $t = {b_q}^p + {d_q}^{1-p} - 1 - p\Delta$ for $m_q = 1$ or $\boldsymbol{x} \in \mathcal{X}_q$ at $t \in ([{a_q}^p + {c_q}^{1-p} - 1, t_{q,*}] - p\Delta)$ for $m_q = 0$ under the control law (7) indicates that ϕ_q is satisfied. Note that Δ only takes effect if $p = 1$ ($\theta = \theta^{s_1}$) to ensure that ϕ_q is satisfied within $[a_q, b_q]$, while for $p = 0$ ($\theta = \theta^{s_2}$) the formula ϕ_{q+1} is directly processed next when ϕ_q is satisfied. Further define $\mathcal{D}_{N+1} := (N+1) \times \Omega'_{N,\boldsymbol{x}} \times T \times \mathcal{Y}_N$ for $T := {b_N}^p + (\sum_{i=1}^{N} d_i)^{1-p} - 1$, which is needed for a technical reason in the proof of Theorem 3. Similarly, define the continuous domain $\mathcal{C}_q$ for $q \in \{1, \ldots, N\}$ as

$$\mathcal{C}_q := \begin{cases} q \times \Omega'_{q,\boldsymbol{x}} \times [0, {b_q}^p + {d_q}^{1-p} - 1 - p\Delta] \times \mathcal{Y}_q & \text{if } m_q = 1 \\ q \times \text{cl}(\Omega'_{q,\boldsymbol{x}} \setminus \mathcal{X}) \times [0, t_{q,*} - p\Delta] \times \mathcal{Y}_q & \text{else,} \end{cases}$$

where cl$(\cdot)$ denotes the closure. Also define $\mathcal{C}_{N+1} := (N+1) \times \Omega'_{N,\boldsymbol{x}} \times [0, T] \times \mathcal{Y}_N$. Finally, the jump and flow sets are

$$D := \cup_{i=1}^{N+1} \mathcal{D}_i$$
$$C := \cup_{i=1}^{N+1} \mathcal{C}_i.$$

The flow map is given by

$$F := \begin{bmatrix} 0 & \big(f(\boldsymbol{x}) + g(\boldsymbol{x})\boldsymbol{u}_q + \boldsymbol{w}\big)^T & 1 & \boldsymbol{0}_7{}^T \end{bmatrix}^T$$

with the control law in (7) as $\boldsymbol{u}_q = -\epsilon_q g^T(\boldsymbol{x}) \frac{\partial \rho^{\psi_q}(\boldsymbol{x})}{\partial \boldsymbol{x}}$ for all $q \in \{1, \ldots, N\}$ and $\boldsymbol{u}_{N+1} = -\epsilon_N g^T(\boldsymbol{x}) \frac{\partial \rho^{\psi_N}(\boldsymbol{x})}{\partial \boldsymbol{x}}$, where ϵ_q corresponds to ϵ based on ϕ_q. By abbreviating $q' := q + 1$, define $\boldsymbol{p}_s(q) :=$

$\begin{bmatrix} q' & \boldsymbol{x}^T & 0 & \Delta_{q'} & t_{q',*} & r_{q'} & \rho_{q',max} & \gamma_{q',0} & \gamma_{q',\infty} & l_{q'} \end{bmatrix}^T$ and finally set the jump map to

$$G := \begin{cases} \boldsymbol{p}_s(q) & \text{if } q \notin \{N, N+1\}, \boldsymbol{z} \in D \\ \begin{bmatrix} N+1 & \boldsymbol{x}^T & \boldsymbol{0}_2^T & \boldsymbol{p}_f{}^T \end{bmatrix}^T & \text{if } q \in \{N, N+1\}, \boldsymbol{z} \in D, \end{cases}$$

with $\Delta_{q'} := \Delta + t$, accumulating the elapsed time. Select $t_{q',*}$ as in (12) and $\rho_{q',max} \in \big(\max(0, \rho^{\psi_{q'}}(\boldsymbol{x})), \rho_{opt}^{\psi_{q'}}\big)$, $r_{q'} \in [0, \rho_{q',max})$ as in the assumptions of Theorem 1 and 2, respectively. The parameters $\gamma_{i,0}$, $\gamma_{i,\infty}$, and l_i need to be chosen as in (9), (10), and (11): $\gamma_{q',0} \in \begin{cases} (\rho_{q',max} - \rho^{\psi_{q'}}(\boldsymbol{x}), \infty) & \text{if } t_{q',*} - p\Delta_{q'} > 0 \\ (\rho_{q',max} - \rho^{\psi_{q'}}(\boldsymbol{x}), \rho_{q',max} - r_{q'}] & \text{if } t_{q',*} - p\Delta_{q'} = 0 \end{cases}$, $\gamma_{q',\infty} \in \Big(0, \min\big(\gamma_{q',0}, \rho_{q',max} - r_{q'}\big)\Big]$, and

$$l_{q'} \in \begin{cases} \mathbb{R}_{\geq 0} & \text{if } -\gamma_{q',0} + \rho_{q',max} \geq r_{q'} \\ -\frac{\ln\left(\frac{r_{q'} + \gamma_{q',\infty} - \rho_{q',max}}{-(\gamma_{q',0} - \gamma_{q',\infty})}\right)}{t_{q',*} - p\Delta_{q'}} & \text{if: } \bullet -\gamma_{q',0} + \rho_{q',max} < r_{q'}, \\ & \quad\ \bullet\ t_{q',*} - p\Delta_{q'} > 0. \end{cases}$$

The initial state is set to $\boldsymbol{z}_0 := \begin{bmatrix} 1 & \boldsymbol{x}_0{}^T & 0 & 0 & t_{1,*} & r_1 & \rho_{1,max} & \gamma_{1,0} & \gamma_{1,\infty} & l_1 \end{bmatrix}^T$. Now, we are ready to state the main result of this section.

Theorem 3: Consider the system (1) and a formula θ as in (3e). The hybrid system $\mathcal{H} := (C, F, D, G)$ results in $r := \min(r_1, \ldots, r_N) < \rho^\theta(\boldsymbol{x}, 0) < \rho_{max} := \min(\rho_{1,max}, \ldots, \rho_{N,max})$, i.e., $(\boldsymbol{x}, 0) \models \theta$, if each ϕ_q in θ is feasible w.r.t. r_q, $\boldsymbol{x}(\Delta_q)$, and $t_{q,*} + |p-1|\Delta_q$.

Proof: The proof can be found in [13]. ■

VI. Simulations

We consider a multi-agent system employing the well-known consensus protocol with additional free inputs. The consensus protocol can be seen as the desire of the group to stay close to each other. Consider M agents where each agent $j \in \{1, \ldots, M\}$ obeys the dynamics $\dot{\boldsymbol{x}}_j = \boldsymbol{v}_j$ with $\boldsymbol{x}_j \in \mathbb{R}^2$. The consensus protocol is then included as $\boldsymbol{v}_j := -\sum_{k \in \mathcal{N}_j} (\boldsymbol{x}_j - \boldsymbol{x}_k) + \boldsymbol{u}_j$ where $\mathcal{N}_j$ denotes the neighborhood of the agent j. Denoting $\boldsymbol{x} := \begin{bmatrix} \boldsymbol{x}_1{}^T & \ldots & \boldsymbol{x}_M{}^T \end{bmatrix}^T$ and $\boldsymbol{u} := \begin{bmatrix} \boldsymbol{u}_1{}^T & \ldots & \boldsymbol{u}_M{}^T \end{bmatrix}^T$, we can express the dynamics as

$$\dot{\boldsymbol{x}} = -(L \otimes I_2)\boldsymbol{x} + \boldsymbol{u}, \tag{13}$$

where L is the graph Laplacian. Comparing (13) with (1) reveals that $f(\boldsymbol{x}) = -(L \otimes I_2)\boldsymbol{x}$ and $g(\boldsymbol{x}) = I_M \otimes I_2 = I_{2M}$, where I_M is the $M \times M$ identity matrix, i.e., Assumption 1 is trivially satisfied. More specifically, assume three agents α_1, α_2, and α_3 with $L := \begin{bmatrix} 1 & -1 & 0 \\ -1 & 2 & -1 \\ 0 & -1 & 1 \end{bmatrix}$. Denote the robot position with $\boldsymbol{x}_j := \begin{bmatrix} x_{j,1} & x_{j,2} \end{bmatrix}^T$ for $j \in \{1, 2, 3\}$. The initial positions are $\boldsymbol{x}_1(0) := \begin{bmatrix} 1.1 & 3.1 \end{bmatrix}^T$, $\boldsymbol{x}_2(0) := \begin{bmatrix} 2 & 0.5 \end{bmatrix}^T$, and $\boldsymbol{x}_3(0) := \begin{bmatrix} 7 & 1.5 \end{bmatrix}^T$. We also have five goal positions A, B, C, D, and E, which are located at $\boldsymbol{p}_A := \begin{bmatrix} 6 & 4 \end{bmatrix}^T$, $\boldsymbol{p}_B := \begin{bmatrix} 1.2 & 9 \end{bmatrix}^T$, $\boldsymbol{p}_C := \begin{bmatrix} 1.2 & 7 \end{bmatrix}^T$, $\boldsymbol{p}_D := \begin{bmatrix} 1.2 & 5 \end{bmatrix}^T$, and $\boldsymbol{p}_E := \begin{bmatrix} 8 & 7 \end{bmatrix}^T$. We use $\big(\|\boldsymbol{x}_j - \boldsymbol{p}_A\|_\infty < c\big) = \big(|x_{j,1} - p_{A,1}| < c\big) \wedge \big(|x_{j,2} - p_{A,2}| < c\big) = \big(x_{j,1} - p_{A,1} < c\big) \wedge \big(-x_{j,1} + p_{A,1} < c\big) \wedge \big(x_{j,2} - p_{A,2} < c\big) \wedge \big(-x_{j,2} + p_{A,2} < c\big)$ to ensure that $\|\boldsymbol{x}_j - \boldsymbol{p}_A\|_\infty = \max(|x_{j,1} - p_{A,1}|, |x_{j,2} - p_{A,2}|) < c$.

The robots are subject to the following sequential tasks: 1) Robot α_1 moves to A within $7 - 10$ seconds. 2) Within the next $10 - 20$ seconds, α_1, α_2, and α_3 move to B, C, and D, respectively. 3) α_1 moves to E within $5 - 15$ seconds. Additionally α_2 and α_3 form a triangular formation. 4) α_2 and α_3 always keep at least a distance of 1 from α_1 and disperse. More specifically, we have: $\theta := F_{[7,10]}(\psi_1 \wedge F_{[10,20]}(\psi_2 \wedge F_{[5,15]}(\psi_3 \wedge \phi_4)))$ with $\psi_1 := \big(\|\boldsymbol{x}_1 - \boldsymbol{p}_A\|_\infty < 0.1\big) \wedge \psi_{Ass.3}$, $\psi_2 := \big(\|\boldsymbol{x}_1 - \boldsymbol{p}_B\|_\infty < 0.1\big) \wedge \big(\|\boldsymbol{x}_2 - \boldsymbol{p}_C\|_\infty < 0.1\big) \wedge \big(\|\boldsymbol{x}_3 - \boldsymbol{p}_D\|_\infty < 0.1\big) \wedge \psi_{Ass.3}$, $\psi_3 := \big(\|\boldsymbol{x}_1 - \boldsymbol{p}_E\|_\infty < 0.1\big) \wedge \big(1 < x_{1,1} - x_{2,1} < 1.2\big) \wedge \big(1 < x_{1,1} - x_{3,1} < 1.2\big) \wedge \big(1 < x_{2,2} - x_{1,2} < 1.2\big) \wedge \big(1 < x_{1,2} - x_{3,2} < 1.2\big) \wedge \psi_{Ass.3}$, and $\phi_4 := G_{[0,12]}\big((1 < x_{1,1} - x_{2,1}) \wedge (1 < x_{2,2} - x_{1,2}) \wedge (1 < x_{1,1} - x_{3,1}) \wedge (1 < x_{1,2} - x_{3,2}) \wedge \psi_{Ass.3}\big)$ with $\psi_{Ass.3} := (\|\boldsymbol{x}\|_\infty < 100)$ to enforce Assumption 3.

The simulation result for the first two formulas, i.e., ψ_1 and ψ_2, are displayed in Fig. 2a and 2b, respectively. For ψ_1, the consensus dynamics bring the agents together, while the performance function γ_1 forces α_1 to approach and reach A. For the second task in Fig. 2b, each agent individually reaches its goals B, C, and D. The third task is shown in Fig. 2c, where the robots initially gather and eventually form a triangular formation, while α_1 approaches E. In Fig. 2d, dispersion of the multi-agent system can be seen. Note that these tasks are achieved successively and we used, for the convenience of the reader, four separate figures. The full trajectory in one figure can be seen in [13, Fig. 2]. To see that time bounds have been respected, Fig. 3 displays the funnels w.r.t. time. The control inputs are bounded and piecewise-continuous, shown in [13, Fig. 4b]. To conclude, θ is satisfied with $r := 0.05 < \rho^\theta(\boldsymbol{x}, 0)$. Note that due to the precision that we chose, e.g., $F_{[7,10]}\big(\|\boldsymbol{x}_1 - \boldsymbol{p}_A\|_\infty < 0.1\big)$, r can not exceed 0.1. We remark that the control law is centralized and that simulations have been performed in real-time, which is possible due to the easy-to-implement feedback control law.

VII. Conclusion

We considered nonlinear systems subject to a subset of signal temporal logic specifications. The imposed transient and steady-state behavior of the prescribed performance control approach was leveraged to satisfy atomic temporal formulas. A hybrid control strategy was then used to ensure that a finite set of atomic temporal formulas is satisfied. A salient feature is that the feedback control law is piecewise-continuous and robust with respect to disturbances and the specification, i.e., the specification is satisfied with a user-defined robustness.

Future work will include the extension of the derived methods to decentralized multi-agent systems with couplings in various forms. In this respect, local and global specifications will be subject of our work, as well as the feasibility of these coupled specifications. Furthermore, an extension of the expressivity, i.e., the signal temporal logic subset under consideration, will be investigated.

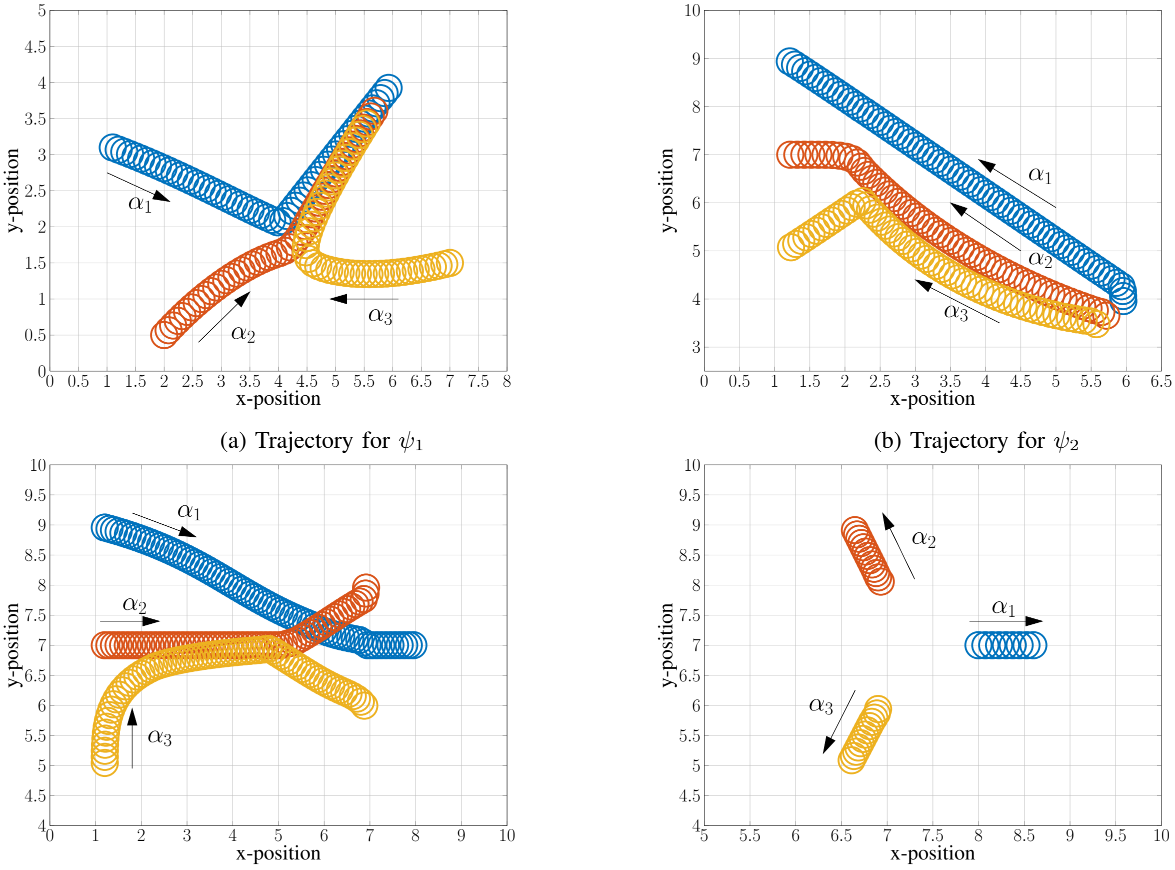

(a) Trajectory for ψ_1

(b) Trajectory for ψ_2

(c) Trajectory for ψ_3

(d) Trajectory for ψ_4

Fig. 2: Trajectories of the three robots.

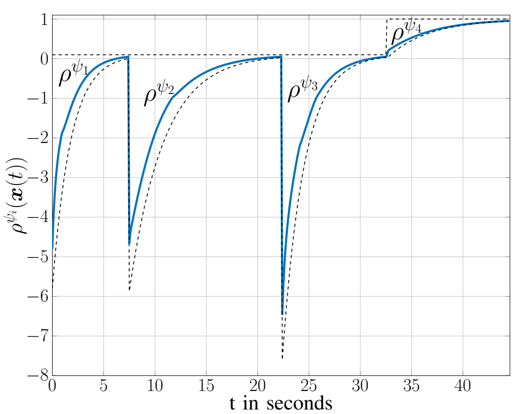

Fig. 3: Error funnel of all four tasks

References

[1] G. E. Fainekos, A. Girard, H. Kress-Gazit, and G. J. Pappas, "Temporal logic motion planning for dynamic robots," *Automatica*, vol. 45, no. 2, pp. 343–352, 2009.

[2] M. Kloetzer and C. Belta, "Automatic deployment of distributed teams of robots from temporal logic motion specifications," *IEEE Transactions on Robotics*, vol. 26, no. 1, pp. 48–61, 2010.

[3] A. Nikou, J. Tumova, and D. V. Dimarogonas, "Cooperative task planning of multi-agent systems under timed temporal specifications," in *American Control Conference (ACC)*. IEEE, 2016, pp. 7104–7109.

[4] C. Baier and J.-P. Katoen, *Principles of model checking*. MIT press, 2008.

[5] C. P. Bechlioulis and G. A. Rovithakis, "A low-complexity global approximation-free control scheme with prescribed performance for unknown pure feedback systems," *Automatica*, vol. 50, no. 4, pp. 1217–1226, 2014.

[6] O. Maler and D. Nickovic, "Monitoring temporal properties of continuous signals," in *Formal Techniques, Modelling and Analysis of Timed and Fault-Tolerant Systems*. Springer, 2004, pp. 152–166.

[7] A. Donzé and O. Maler, "Robust satisfaction of temporal logic over real-valued signals," in *Proceedings of the 8th international conference on Formal modeling and analysis of timed systems*. Springer-Verlag, 2010, pp. 92–106.

[8] L. Lindemann and D. V. Dimarogonas, "Robust motion planning employing signal temporal logic," in *2017 American Control Conference (ACC)*. IEEE, 2017, pp. 2950–2955.

[9] V. Raman, A. Donzé, M. Maasoumy, R. M. Murray, A. Sangiovanni-Vincentelli, and S. A. Seshia, "Model predictive control with signal temporal logic specifications," in *Decision and Control (CDC), 2014 IEEE 53rd Annual Conference on*. IEEE, 2014, pp. 81–87.

[10] S. Sadraddini and C. Belta, "Robust temporal logic model predictive control," in *2015 53rd Annual Allerton Conference on Communication, Control, and Computing (Allerton)*. IEEE, 2015, pp. 772–779.

[11] Z. Liu, J. Dai, B. Wu, and H. Lin, "Communication-aware motion planning for multi-agent systems from signal temporal logic specifications," in *2017 American Control Conference (ACC)*. IEEE, 2017, pp. 2516–2521.

[12] R. Goebel, R. G. Sanfelice, and A. R. Teel, *Hybrid Dynamical Systems: modeling, stability, and robustness*. Princeton University Press, 2012.

[13] L. Lindemann, C. K. Verginis, and D. V. Dimarogonas, "Prescribed performance control for signal temporal logic specifications," *arXiv preprint arXiv:1703.07094*, 2017.